All-Optical Fiber-Cantilever Beam-Deflection Magnetometer: Detection of Low Magnetic Field and Magnetization Measurement

Partha Roy Chaudhuri and Somarpita Pradhan

Abstract All-optical fiber-cantilever beam deflection configuration using an optimized composition of cobalt doped nickel ferrite nanoparticles coated single-mode optical fiber cantilevers is demonstrated. Initially, a fiber-double-slit interferometer arrangement using coated fiber-cantilever-deflection is devised to detect the surrounding magnetic field by precisely measuring the changes in interference fringe-width. A theoretical platform is developed to model the fiber-cantilever deflection which in turn predicts magnetization value of the probe sample. In order to explore higher sensitivity, *etched* single-mode fiber cantilever is incorporated in double-slit arrangement and a marked improvement is achieved. Next, we refined the experiment by tracking the amplitude-modulation of propagating light through fiber-to-fiber coupling cantilever deflection-transmission arrangement which showed increased sensitivity further. In a series of experiments starting with single cantilever transmission technique, we ended up with a model of cascaded cantilevers to sense very low order (~ 1 *m*T) magnetic field. Developed theoretical model fairly predicts experimentally obtained results, in particular, the magnetization of the probe sample. We demonstrate that the scheme is capable of reproducing magnetization data obtained from high precision SQUID measurement. Finally, Sagnac loop assisted cascaded cantilever configuration is realized experimentally to establish the repeatability and more stable response of cascaded cantilever scheme. All our experimental configurations are all-optical with minimum system complexities. These results are new and will provide guideline and understanding towards designing fiber-optic low-magnetic field sensors $\sim m$T.

P.R. Chaudhuri (✉) · S. Pradhan
Indian Institute of Technology Kharagpur, Kharagpur, West Bengal 721302, India
e-mail: roycp@phy.iitkgp.ernet.in

S. Pradhan
e-mail: somarpita.lbc@gmail.com

I. Bhattacharya et al. (eds.), *Advances in Optical Science and Engineering*,
Springer Proceedings in Physics 194, DOI 10.1007/978-981-10-3908-9_15

1 Introduction

The advancement in technology in the area of Photonics is very rapid compared to other technologies. Enormous application of photonic devices offers us an instance of the significance of this emerging discipline. Now-a-days, dielectric waveguide structures cover a large area in the field of fundamental research as well as in industry application. One outcome of these photonic waveguides in the form of optical fibers has a major role not only in communication but also in the development of different type of sensors. The fiber optic sensing offers some unique features which make it prominent among other sensing methods. Some of the essential motives for the recognition of optical fiber based sensor structures are small length, light weight, immunity to electromagnetic interference (EMI), capability of far field sensing, dielectric composition, higher sensitivity and multiplexing operation. Using fiber-optic sensors, one can measure different physical or chemical parameters for example voltage, magnetic field, temperature, humidity, strain, pH, rotation and so forth. Information about the measurand is conveyed in all optical fiber sensors by way of alternating polarization, intensity, frequency, phase or a combination of the above. Fiber optic sensors are often grouped into two basic classes referred to intrinsic and extrinsic sensors. In intrinsic fiber optic sensor, the fiber acts as active sensing area whereas in extrinsic fiber sensors, the fiber simply transmits light to and from the sensing medium.

Though the measurement of low magnetic field attracted huge research interest for decade, most of the reported measurement schemes either involve measurement of induced longitudinal strain caused by applied magnetic field [1] or require complex hardware or signal processing system [2]. A relatively new technology, cantilever-beam deflection, has attracted the research attention in recent years in the area of sensing and device applications [3–5]. Because of the high precision and scalability, the cantilever techniques are most often used in environmental monitoring, temperature, humidity, UV radiation sensing and also in medical, chemical, biochemical measurements. Consequent upon these features, we emphasized on devising a fiber-optic cantilever-beam deflection based sensor configuration which is capable of detecting low order magnetic field with minimum system complexity. The proposed scheme would be suitable for remote sensing, in particular at hazardous environment where electrical probes cannot be deployed. For designing such type of sensors, we need to at first identify a proper probe magnetic material. Spinel type oxide, Cobalt-doped nickel ferrite ($Ni_{0.97}Co_{0.03}Fe_2O_4$) was reported in literature for its exceptionally high magnetic properties [6] and was used by M. Sedlar et al. for devising a Mach-Zehnder interferometer type magnetic field sensor [7]. Consequent upon these findings, Cobalt-doped nickel ferrite ($Ni_{0.97}Co_{0.03}Fe_2O_4$) material was chosen as our probe magnetic material. In the following sections, in brief we describe our preparation methodology of probe magnetic material, end characterization results and chronology of developments of magnetic field sensing experimental set-ups based on cantilever deflection.

2 Probe Material Preparation Method and Characterisation

Among different routes, we adopted sol-gel method for sample preparation due to its capability of producing high purity products, low processing temperature and low cost. The material was prepared using nitrate salts of iron [$Fe(NO_3)_3 \cdot 9H_2O$], nickel [$Ni(NO_3)_3 \cdot 6H_2O$] and cobalt [$Co(NO_3)_2 \cdot 6H_2O$] [8]. Firstly, solution of iron nitrate in ethylene glycol was prepared at temperature 70 °C and kept in an ultrasonic cleaner. Then, nickel and cobalt nitrates were added in preheated 2-methoxyethanol (2-MOE) maintaining the stoichiometry. This solution was then mixed with previously prepared iron nitrate solution and stirred at 70 °C until gelation. Finally, the prepared sample was dried and grinded properly and annealed at 600 °C for 3 h and various characterization processes were performed. The crystalline structure of the probe material ($Ni_{0.97}Co_{0.03}Fe_2O_4$) was investigated by X-ray diffraction (XRD) analysis using CuK_α source (wavelength 1.54 Å) at room temperature. The lattice constant was estimated to be ~8.35 Å. We also evaluated coercive field (H_C) value of the magnetic probe material and reported [9] value was 175.50 Oe.

3 Fiber-Cantilever Deflection Setups and Magnetic Field Sensing

3.1 Interferometric Configuration

As an initial step, we attempted a fiber double-slit interferometer experiment where two exit fibers were placed adjacent to each other by making cantilevers of desired length to act as twin-source of interference (see Fig. 1).

3.1.1 Configuration Details and Result

Light from a HeNe laser was coupled into one input of a 3 dB coupler (at 632.8 nm) which acts as a beam-splitter and splits light equally into two output

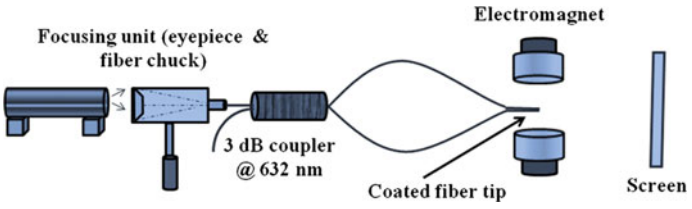

Fig. 1 Schematic of interferometric configuration [9]

ports. One of these ports was coated with the cobalt-doped nickel-ferrite particles and placed parallel with other one making a cantilever of length 2.0 cm. Among different coating methods, we adopted a gluing technique of attaching magnetic nanoparticles over the fiber surface that showed high response [10] in low field.

In presence of magnetic field, due to induced magnetization and consequent bending of coated fiber, separation between two exits fiber ports (twin-source) increases. This leads to dynamic change in the fringe-width (β) at various fields as observed at a screen placed at a large distance as given by

$$\beta = \frac{\lambda D}{d} \tag{1}$$

Here, D denotes the distance from the sources to the screen and the separation of two interfering sources is expressed by d. Experimental result in terms of fringe with variation is shown in Fig. 2(left).

3.1.2 Etching Single-Mode Fiber as Cantilever

As the etched fibers are recognized for their flexible nature and anticipated for higher response, we next introduced etched fiber cantilever in the setup. Single-mode fibers (S405-XP) were etched [11] by using HF 40% pure (MERCK) solution at room temperature (300 K). The etching rate was estimated to be 2.27 μm/min. An optimized etched fiber with diameter 50 μm ± 5 μm coated with probe magnetic material having the same coated fiber length of 1.2 (±0.1) cm (as used for normal fiber case) was incorporated in the interferometric

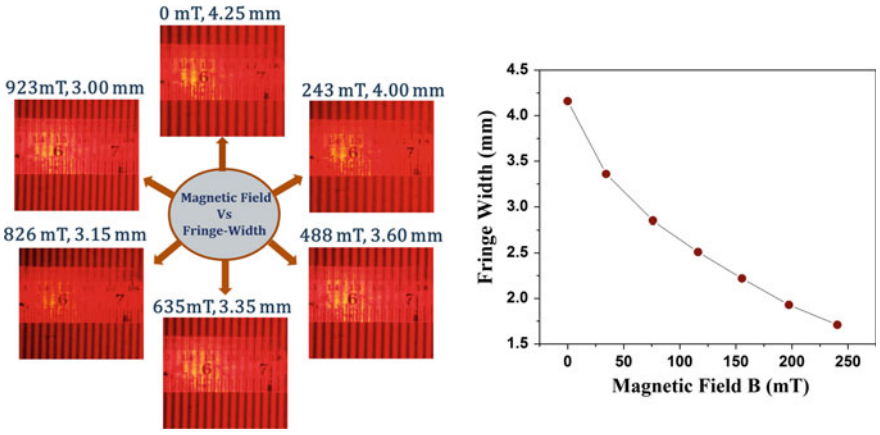

Fig. 2 Recorded photographs of variation of fringe-width as a function of magnetic field using normal coated single-mode fiber (S405-XP) (*left*) and measured fringe-width as a function of magnetic field using etched coated fiber (*right*) [9]

configuration. As expected, sensitivity was seen to improve noticeably. Fringe-width variation results for etched fiber cantilevers (coated fiber thickness 0.12 mm) are shown in Fig. 2(right) which nicely depicts the enhanced sensitivity obtained in this modified scheme.

3.1.3 Model of Fiber Cantilever Deflection: Determination of Magnetization of Probe Material

Magnetization (M) of the sample for a constant magnetic field (B) can be estimated using the basic torque (τ_m) relation [12]:

$$\tau_m = V_m M \times B \tag{2}$$

Here, volume of magnetic particles used is denoted by V_m. For fiber cantilever, torque experienced due to the external magnetic field is balanced by the internal bending moment (EI/R) of the fiber. E and I represent the elastic modulus and the geometrical moment of inertia of the cantilever substrate respectively. By equating these two, for the case of distributed torque acting over the coated length ($b - a$) of the fiber [see Fig. 3(left)], deflection (Δ) can be expressed as [13],

$$\Delta = \frac{V_m BM}{6EI}\left[\frac{(b-z)^3}{(b-a)} - 3(b+a)(b-z) + 2b(b+a) - a^2\right] \tag{3}$$

So, deflection of the fiber end with cantilever length b ($z = b$ point) will be given by [9]

$$\Delta = \frac{V_m BM}{6EI}[2b(b+a) - a^2] \tag{4}$$

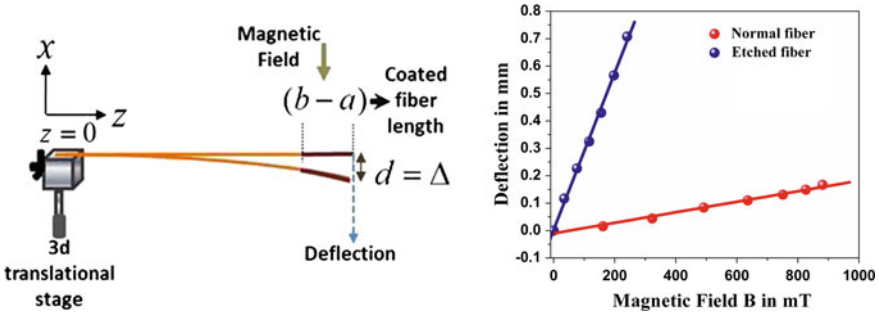

Fig. 3 Schematic of bending of the fiber due to application of magnetic field with specified co-ordinate (*left*) and variation of estimated deflection for normal and etched coated fiber obtained from interferometric configuration (*right*) [9]

Table 1 Magnetization values of probe material obtained from SQUID measurement and interferometric configuration [9]

Magnetic field (Gauss)	Magnetization M (emu/cc) from SQUID data $\times 10^{-3}$	Magnetization M (emu/cc) from experiment $\times 10^{-3}$
1614	347	582
3230	752	801
4915	1130	1005
6355	1420	1018
7510	1920	1026
8260	2070	1061
8810	2150	1115

We calculated deflection of normal and etched fiber tips under calibrated magnetic field using (1) and these are shown in Fig. 3(right). Improved sensitivity of cantilever deflection of the etched fiber is evident from the plot. These calculated deflection values for normal coated fiber cantilever with 0.32 mm thick coating were incorporated in (4) to extract magnetization of the magnetic material (listed in Table 1). In the table, the magnetization data obtained from SQUID measurement is also quoted to appreciate the performance of this experiment which fairly predicts the order of magnitude of the magnetization value under different field strength.

3.2 Fiber-to-Fiber Cantilever Transmission Arrangement

In this configuration, magnetic field was measured by modulating the amplitude of propagating light through misalignment zone between two cascaded optical fibers (butt-coupled) one being the coated deflection cantilever.

3.2.1 Single Cantilever Transmission Configuration

In this arrangement, light (@632.8 nm) propagating through single-mode fiber experiences a transverse misalignment (Fig. 4) at the end coated fiber port (acting as the cantilever in a magnetic field) while butt-coupled to a similar fiber.

Cantilever length is varied from 2.0 to 3.0 cm in order to extract optimized sensitivity. Intensity of coupled light into the receiving fiber as a function of gradually increasing or decreasing magnetic field was recorded to measure the magnetic field causing deflection of the coated fiber-tip. Power variation experimental result is shown in Fig. 5(left) for varying cantilever length. It is clearly seen from the results that larger cantilever length showed higher sensitivity but dynamic range of operation reduces. Thus optimization of cantilever configuration owes much to given range. We then reconfigured the set-up by replacing the fiber cantilever with etched coated single mode fiber with fiber diameter 50 μm ± 5 μm.

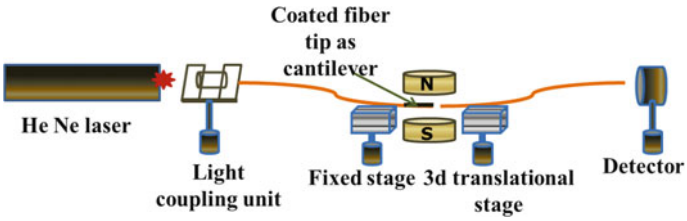

Fig. 4 Schematic of single cantilever transmission configuration [9]

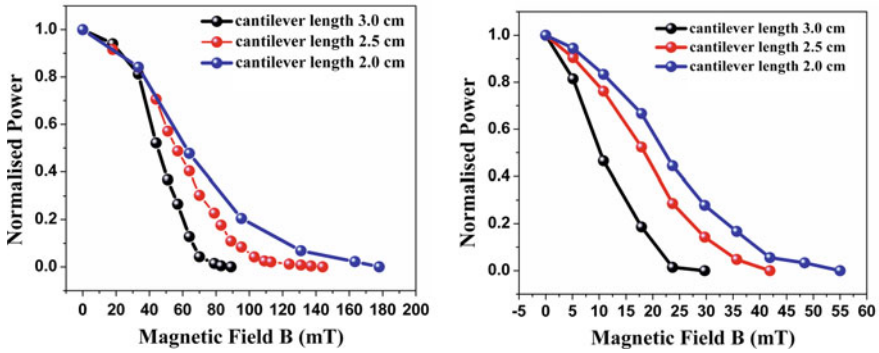

Fig. 5 Transmitted power variation with magnetic field using single-mode fiber (S405-XP) (*left*) and etched fiber (*right*) [9]

Keeping the coating length same (1.2 (±0.1) cm), response of the etched port was recorded for different cantilever lengths. Modified system also establishes enhanced sensitivity of the bigger cantilever length (3.0 cm). We observed reversible and repeatable response for both the cases of normal and etched fiber cantilever. Improved response of the modified scheme is shown in Fig. 5(right).

3.2.2 Double Cantilever Transmission Configuration

Based on the former work, to realize better sensitivity without chemical etching process, we then reconfigured the single cantilever model to double cantilever transmission scheme. By the term "double cantilever", we describe a configuration that involves two successive transverse misalignment zones (see Fig. 6) unlike the single cantilever scheme.

We maintained the coated fiber length as 1.2 ± 0.1 cm and cantilever length (3.0 cm) throughout the experiment as these are the optimized values obtained from the single cantilever arrangement. In this double cantilever set-up, one transverse off-set (between fiber 1 and 2) followed by another (between fiber 2 and 3) result in rapid decrement in transmitted power which makes the configuration more sensitive to weak magnetic field compared to single cantilever scheme.

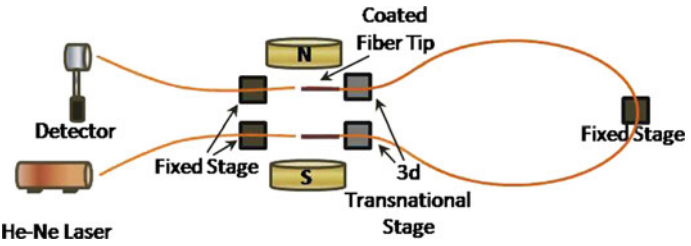

Fig. 6 Schematic of double cantilever transmission configuration

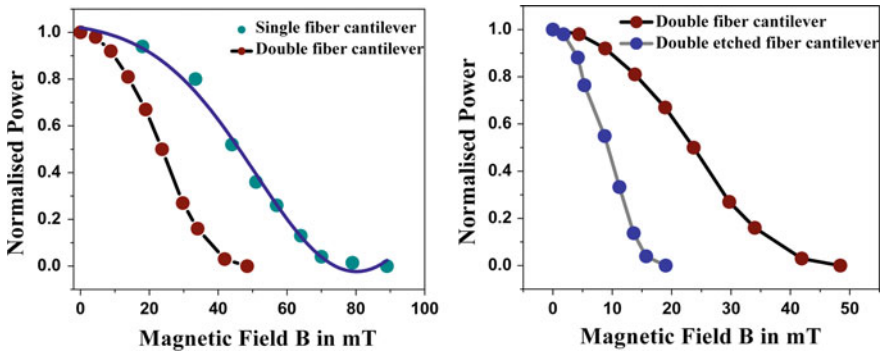

Fig. 7 Comparison between response of single and double cantilever configuration (*left*) in a calibrated magnetic field and response of double cantilever transmission configuration using both normal and etched coated fiber cantilevers (*right*)

We recorded the light intensity coupled into the last receiving fiber as a function of varying magnetic field. The experimentally obtained data are plotted in Fig. 7 (left). We also placed the results obtained from single cantilever setup to distinguish the improved response of double cantilever [14]. Response of the etched fiber (60 μm ± 5 μm) cantilevers is also plotted in this figure (Fig. 7(right)). This scheme is capable of detecting magnetic field as low as 1 *m*T.

3.2.3 Theoretical Model of Fiber-to-Fiber Transmission: Estimation of Deflection

Considering the normalized Gaussian fundamental modes of two single-mode fibers that have transverse offset d_1 as

$$\psi_1(x,y) = \sqrt{\frac{2}{\pi}}\frac{1}{w_1}e^{-\frac{(x^2+y^2)}{w_1^2}} \quad \text{and} \quad \psi_2(x,y) = \sqrt{\frac{2}{\pi}}\frac{1}{w_2}e^{-\frac{\left[(x-d_1)^2+y^2\right]}{w_2^2}} \tag{5}$$

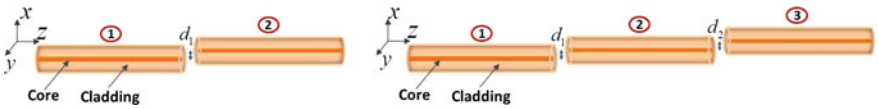

Fig. 8 Schematic of transverse misalignment between two (*left*) or three (*right*) optical fibers

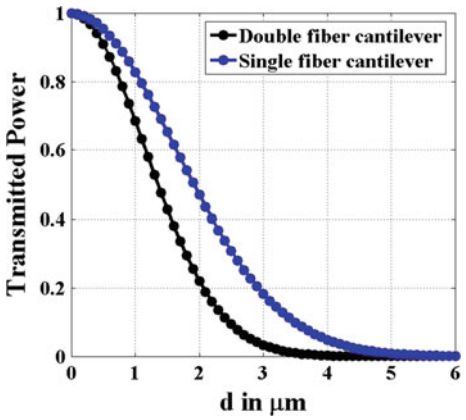

Fig. 9 Transmitted power variation profile with increasing transverse misalignment for both single and double fiber cantilever configuration using S405-XP single mode fibers

in the direction of x (as shown in Fig. 8) and propagating along z, the fractional transmitted power to the second receiving fiber from the first is obtained from the overlap integral [15]

$$T_{12} = \left| \int_{-\infty}^{+\infty} \int_{-\infty}^{+\infty} \psi_1 \psi_2^* dx dy \right|^2 = \left(\frac{2w_1 w_2}{w_1^2 + w_2^2} \right)^2 e^{-\frac{2d_1^2}{w_1^2 + w_2^2}} \tag{6}$$

Here, w_1 and w_2 are the spot sizes of fundamental modes of fiber 1 and fiber 2 respectively.

Equation (6) can be adopted for three fiber-system incorporating two successive transverse misalignments of the fibers:

$$T_{13} == \left(\frac{4w_1 w_2^2 w_3}{\left(w_1^2 + w_2^2\right)\left(w_2^2 + w_3^2\right)} \right)^2 e^{-2\left[\frac{d_1^2}{w_1^2 + w_2^2} + \frac{d_2^2}{w_2^2 + w_3^2}\right]} \tag{7}$$

For three identical optical fibers imposing the condition $d_1 = d_2 = d$, transmitted power to third fiber will be:

$$T = e^{-\frac{2d^2}{w^2}} \tag{8}$$

The transmitted power variation profile for the both single and double misalignment cases involving identical single mode fibers (S405-XP) having mode field diameters 4.6 μm ± 0.5 μm at 632 nm wavelength is plotted in Fig. 9.

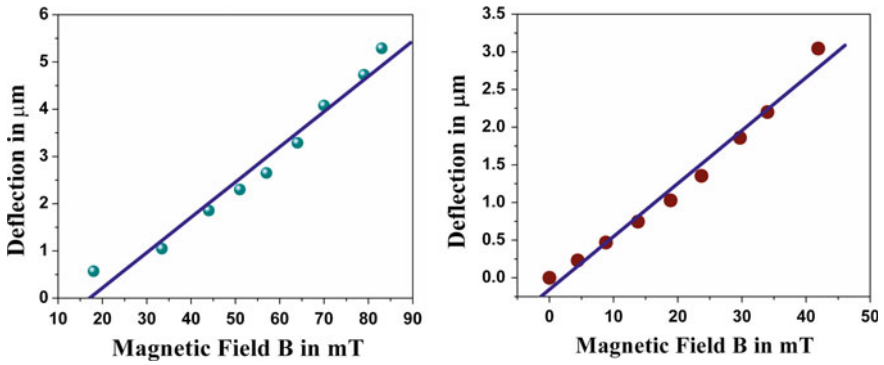

Fig. 10 Deflection values at different magnetic field for both single (*left*) and double (*right*) cantilever transmission

Sensitivity can be tuned further by realizing the cascaded model. For n such cascaded misalignments,

$$T = e^{-\frac{nd^2}{w^2}} \tag{9}$$

Equation (9) clearly indicates the effect of cascading in terms of sensitivity.

3.2.4 Determination of Magnetization of Probe Material

Deflection (Δ) of the coated fiber-tip due to the applied magnetic field was then calculated by fitting the experimental results with the theoretical model and depicted in Fig. 10 for both single and double cantilever cases for cantilever length 3.0 cm. Estimated deflections values were used to calculate the magnetization (M) of the probe sample. For our case of single and double cantilever configurations with 0.47 mm and 0.56 mm of coated fiber thickness respectively, magnetization values are listed in Table 2. We have used the value of E = 70 GPa and $I = \pi D^4/64$, where D is the diameter of the fiber (substrate material).

3.3 *Sagnac Loop Assisted Cascaded Cantilever Configuration*

We next implemented a Sagnac loop assisted cascaded cantilever configuration in order to realize two exactly identical cantilever paths for two opposite (forward and

Table 2 Magnetization of probe material obtained from both single and double cantilever transmission configuration

Single cantilever		Double cantilever	
Magnetic field (Gauss)	Magnetization M (emu/cc) from experiment $\times 10^{-3}$	Magnetic field (Gauss)	Magnetization M (emu/cc) from experiment $\times 10^{-3}$
180	32.3	43	36.9
334	32.4	88	37.4
440	43.0	138	38.0
510	46.0	189	38.2
570	48.1	237	40.1
640	52.4	297	44.0
700	59.4	340	45.5
790	61.0	419	57.1

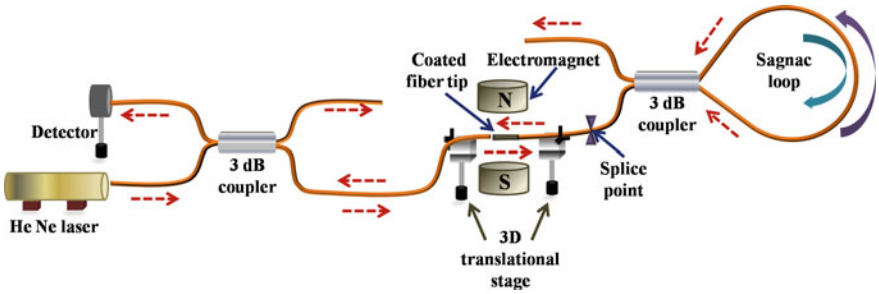

Fig. 11 Schematic of Sagnac loop assisted cascaded cantilever configuration

backward) propagating light. In this configuration, laser light was coupled to one input of a 3 dB coupler while the other input was used to detect transmitted light as shown in Fig. 11.

One output port of the coupler acts as the transmitting/receiving end of the cantilever stage with a Sagnac loop mirror using a second 3 dB coupler. The cantilever (coated fiber length 1.2 ± 0.1 cm) is formed at the input port of the Sagnac loop made by splicing the two output ports of a 3 dB coupler. Due to the fiber-mirror characteristics of Sagnac loop, light traveling through the misalignment zone (caused by external magnetic field) traverses the identical path twice leading to double the response as detected from the backward propagating light through the first 3 dB coupler. The response of this scheme as intensity variation with applied magnetic field is depicted in Fig. 12(left). Then, we reconfigured our set-up using etched coated fiber cantilevers and their response in terms of power variation is depicted in Fig. 12(right).

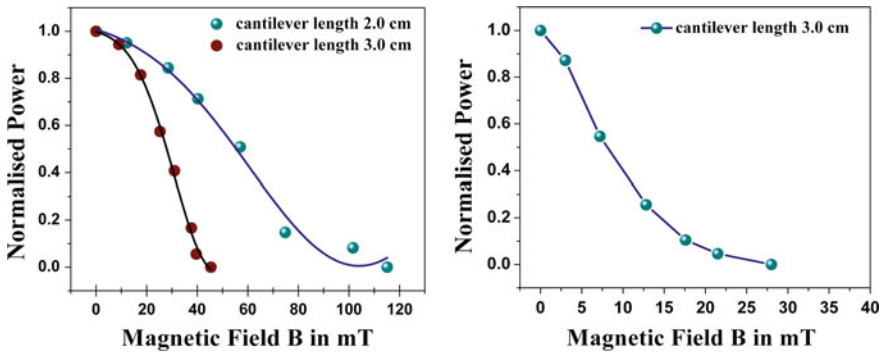

Fig. 12 Response of sagnac loop assisted cascaded cantilever configuration using normal (*left*) and etched (*right*) fibers

4 Conclusion

In this article, we detailed our experimental research aimed at devising a weak magnetic field detection system which is all-optical, and particularly useful in electrically hazardous environment. The series of experimental studies began with interferometric setup of measuring surrounding low-magnetic field by tracking the dynamic change in fringe pattern. Improvement in response was achieved by incorporating etched coated fiber tip. Then, modulation of light-beam propagating through single-mode optical fiber was devised utilizing the transverse misalignment between two butt-coupled optical fibers, one being a coated cantilever. This model was reconfigured as double cantilever transmission arrangement with a visible improvement in sensitivity. A theoretical platform is provided which nicely interprets the experimental data. Magnetization of the probe sample is also calculated using our theory and validated by quoting SQUID measurement data. Our approach is capable of detecting magnetic field ~ 1 *m*T or even lower without any system complexity or involving any complex circuit. Sagnac loop assisted double-pass identical cantilever scheme is demonstrated for higher sensitivity. These results could be helpful for developing low magnetic field detection schemes.

Acknowledgements The authors sincerely acknowledge BRNS, Govt. of India for the financial support to carry out this research.

References

1. Dai, Y., Yang, M., Xu, G., and Yuan, Y., "Magnetic field sensor based on fiber Bragg grating with a spiral microgroove ablated by femtosecond laser," Opt. Expr. 21, 17386–17391 (2013).
2. Lenz, J., and Edelstein, A. S., "Magnetic sensors and their applications," IEEE Sens. 6, 631–649 (2006).

3. Koch, R. *et al.*, "Perpendicular magnetic fields in cantilever beam magnetometry," J. Appl. Phys. 96, 2773–2778 (2004).
4. Duc, T. C., *et. al.*, "Piezoresistive cantilever beam for force sensing in two dimensions," IEEE Sens. 7, 96–104 (2007).
5. Kumar, A., *et. al.*, "Cantilever based MEMS pressure sensor using different piezoelectric materials: a comparative study," IJEDR 2, 4022–4026 (2014).
6. Dung, N. K., and Tuan, N. H., "The effect of cobalt substitution on structure and magnetic properties of nickel ferrite," VNU Journal of Science, Mathematics-Physics 25, 153–159 (2009).
7. Sedlar, M. *et al*, "Optical fiber magnetic field sensors using magnetostrictive jackets," Sens. Actu. A 84, 297–302 (2000).
8. Sedlar, M. *et al,* "Preparation of cobalt nickel ferrite films on optical fibers by dip-coating", Ceram. Int. 21, 21–27 (1995).
9. Pradhan, S., and Chaudhuri, P. R., "Experimental demonstration of all-optical weak magnetic field detection using beam-deflection of single-mode fiber coated with cobalt-doped nickel ferrite nanoparticles," Appl. Opt. 54, 6269–6276 (2015).
10. Yang, M., Dai, J., Zhou, C., and Jiang, D., "Optical fiber magnetic field sensors with TbDyFe magnetostrictive thin films as sensing materials," Opt. Expr. 17, 20777–20782 (2009).
11. Kumar, A.*et al.*, "Optimize etching based single mode fiber optic temperature sensor" Int. J. Eng. Res. Appl. 4, 4–8 (2014).
12. Weber, M., Koch, R., and Rieder, K. H., "UHV Cantilever Beam Technique for Quantitative Measurements of Magnetization, Magnetostriction, and Intrinsic Stress of Ultrathin Magnetic Films," Phys. Rev. Lett. 73, 1166–1169 (1994).
13. Adhikari, R.*et al.*, "The cantilever beam magnetometer: a simple tool for characterization" Am. J. Phys. 80, 225–231 (2012).
14. Pradhan S. and Chaudhuri P. R., "Performance of Low Magnetic Field detection using Double Cantilever Fiber-Beam Deflection-Transmission Configuration," JSAP-OSA Joint Symposia, Sept. 13–16, 2015.
15. Ghatak. A., and Thyagarajan, K., "Introduction to Fiber Optics," Cambridge University Press, Reprint 2011.